crystals

MDPI

Article

Solid Phase and Stability Investigation of a Co-Crystal in the L-Valine/L-Leucine System

Vico Tenberg [1,*], Matthias Stein [2] and Heike Lorenz [1]

[1] Physical and Chemical Foundations of Process Engineering Group, Max Planck Institute for Dynamics of Complex Technical Systems, Sandtorstrasse 1, 39106 Magdeburg, Germany; lorenz@mpi-magdeburg.mpg.de
[2] Molecular Simulations and Design Group, Max Planck Institute for Dynamics of Complex Technical Systems, Sandtorstrasse 1, 39106 Magdeburg, Germany; matthias.stein@mpi-magdeburg.mpg.de
* Correspondence: tenberg@mpi-magdeburg.mpg.de

Abstract: Some amino acid systems are known to exhibit solid solution and/or co-crystal behavior upon crystallization, which significantly affects their phase diagrams and complicates the design of their purification processes. Such behaviors are observed in the L-valine/L-leucine system. In this work, the formation and stability of a 3:1 co-crystal of the two amino acids (designated as V_3L) is further investigated. To accomplish the formation, liquid-assisted grinding, slurry equilibration, and sublimation experiments were performed and analyzed via HPLC and PXRD. Additionally, periodic DFT calculations were used to calculate lattice energies and determine the thermodynamics of possible solid phases. Experimental results show a clear metastability of the investigated V_3L co-crystals when compared to its stable solid solution. The calculations underline the metastability and the possible formation of continuous solid solutions between L-valine and L-leucine since lattice energy differences between pure amino acids and mixed compositions are negligible. This previously unknown phase behavior can be used to assess the influence of V_3L on the amino acid purification process and provides a basis for investigating similar systems with small energy differences between pure and mixed compositions in future studies. In addition, it demonstrates the particular variability of solid phases and their relationships in such simple but biologically important amino acid systems.

Keywords: amino acids; co-crystals; metastability; L-leucine; L-valine; lattice energy; periodic DFT

Citation: Tenberg, V.; Stein, M.; Lorenz, H. Solid Phase and Stability Investigation of a Co-Crystal in the L-Valine/L-Leucine System. *Crystals* **2023**, *13*, 1542. https://doi.org/10.3390/cryst13111542

Academic Editor: Abel Moreno

Received: 28 September 2023
Revised: 20 October 2023
Accepted: 23 October 2023
Published: 27 October 2023

1. Introduction

The phase behavior of a given system is of utmost importance for the design of efficient and optimal crystallization processes. Thereby, not only solubility [1] but also the resulting solid phases, such as co-crystals [2], polymorphs [3], and solid solutions [4], are relevant. For example, for amino acids, there are multiple studies observing the polymorphic behavior of L-glutamic [5] and L-aspartic [6] amino acids while also observing solid solution formation in their mixtures [7]. Additionally, co-crystals and solid solutions were found in the L-isoleucine/L-valine and L-leucine (L-Leu)/L-valine (L-Val) systems [2,8]. These systems are shown to form a V_2I and V_3L co-crystal consisting of two or three molecules of L-Val and one molecule of L-isoleucine or L-Leu in the unit cell, respectively. Such non-equimolar molecular compounds in amino acid systems are exceedingly rare and are therefore only scarcely investigated [8]. The L-Val/L-Leu system was extensively studied in our previous works [9–11], verifying the formation of solid solutions. While V_3L was not the focus of these studies, it was only accidentally observed when crystallized from various solvent compositions and conditions. Further, investigation in these studies indicated the metastability of the V_3L co-crystal. A number of additional studies regarding the L-Val/L-Leu system found in the literature [12–14] do not describe the formation of a V_3L co-crystal. In [14], an unknown solid phase was observed in this system, but it was not further specified. This signifies the need for deeper investigations of the nature of the V_3L co-crystal and, thus, its influence on potential purification processes in the related system.

For this, various experimental studies such as liquid-assisted grinding, slurry equilibration based on prior solubility data sets, and sublimation were performed and analyzed via high-performance liquid chromatography (HPLC) and powder X-ray diffraction (PXRD).

To further validate the metastability of V_3L, periodic density functional theory (DFT) calculations were used to calculate lattice energies of L-Val and L-Leu co-crystals at various compositions and the pure amino acids to obtain insight into the energetically preferred solid phase. The magnitude of intermolecular interaction in organic molecular crystals from Density Functional Theory (DFT) can be compared to experimental thermodynamically corrected heats of sublimation. The C21 and X23 benchmark sets are available to assess the accuracy of computational means [15–19]. The 'lattice energy' is the energy of stabilization of the molecule in the solid vs. the fully relaxed isolated molecule in the gas phase. For amino acids, the calculated lattice energies were used to estimate the relative solubilities of enantiopure and racemic crystal forms [20]. Geatches et al. obtained a deviation from the experiment of 16 kJ/mol and 19 kJ/mol for different DFT dispersion correction models for lattice energies of amino acids with an increasing number of Cα atoms (1 to 4 carbon atoms, glycine to isoleucine) [21]. Crystallization-based approaches to produce solid solutions of hydrophobic amino acid residues [22,23] have shown that various molecular compositions can easily be obtained. With only minor changes in unit cell dimensions and molecular conformations, the basic amino acid hydrogen-bonded chains remained unchanged compared to the pure amino acid structures. For co-crystals of L-Leu/L-Val, CCDC entries LENGAP/LANGAP01/LENGAP02 with non-stochiometric compositions indicate the formation of solid solutions. However, the structural disorder introduced upon co-crystallization does not affect the strong intermolecular interactions. Therefore, we here focus on the recently identified V_3L co-crystal from [8] with the CCDC reference LENGAP02.

In the following, experimental procedures and theoretical background will be explained. The resulting data will be discussed and compared with simulation results, and finally, a conclusion will be presented. With it, this work aims to extend the existing knowledge and explain the unusual behavior of the particular co-crystal V_3L by investigating its formation and especially its stability.

2. Experimental Section

2.1. Chemicals

The amino acids L-Val and L-Leu of 98.8 and 100.3% purity (relative to reference), respectively, were supplied by Iris Biotech GmbH. HPLC grade ethanol (>99.7% purity) was obtained from VWR Chemicals. These chemicals were used as received without further purification. Water was purified using a Millipore 40 filter (18.2 MΩ cm, total organic carbon (TOC): 3ppb).

2.2. Experimental Procedures

During this work, comprehensive experiments were conducted to investigate various influences and gather data sets of different perspectives on the L-Val/L-Leu system. For investigation of the V_3L compounds' behavior and stability in the presence and absence of solvents, experiments on crystallization under equilibrium and out-of-equilibrium conditions were run. These included solubility measurements of the system components and their mixtures in water and various water/ethanol mixtures, mechanochemical dry and liquid-assisted grinding of the system components and their mixtures, and slurry equilibration experiments. Further, sublimation studies were performed. The various procedures applied are detailed below.

Solubility measurements: Solubilities of L-Val and L-Leu amino acids in water and water/antisolvent systems were measured in previous works [9–11]. Nevertheless, we see it as beneficial to this work to again explain the experimental procedure here. Physical mixtures of varying ratios were prepared and completely dissolved in a known amount of water at elevated temperatures. If solubilities in water were measured, the solution was

partially evaporated in a rotary evaporator and transferred into a separate vial once the first crystals were observed. To initialize crystallization in experiments aimed to determine solubility in mixed solvents, a specific amount of antisolvent was added to the solution. The resulting suspensions were sealed and stirred continuously in a double-jacketed vessel whose temperature was controlled by a thermostat. Thus, the samples were kept at a constant temperature for at least 72 h before a syringe and a syringe filter (pore size 4 µm) were used to sample the liquid phase for HPLC measurement. After liquid phase sampling, the remaining suspension was filtered via vacuum filtration (pore size 12–16 µm). The resulting solid phase was dried overnight in a vacuum oven at 40 °C and subsequently used in HPLC and PXRD analysis.

Mechanochemical grinding of amino acids: In an attempt to produce the V_3L compound, mixtures of L-Val and L-Leu were ground using a grinding mill Retsch *MM400*. For this, small amounts (~1 g) of the amino acid mixture, with a molar composition L-Val:L-Leu = 3:1, were ground at 25 Hz in a 10 mL vessel containing two stainless steel balls (Ø = 10 mm). The mixtures were ground for various durations and liquid-assisted via the addition of a solvent ranging from a 0 to 0.6 µL mg^{-1} sample. Afterwards, the samples were dried in a vacuum chamber overnight. The samples were analyzed via PXRD and HPLC before and after grinding to detect any change in the solid phase identity and structure or composition.

Slurry equilibration experiments: Two samples, (1) the V_3L compound, which was produced by mechanochemical grinding, and (2) a 50/50 wt.% mixture of sample (1) and a molar 3:1 L-Val:L-Leu physical mixture, were added to a saturated liquid phase containing L-Val and L-Leu in the corresponding equilibrium composition. The mixtures were stirred, manually shaken two times a day and kept at 25 °C for three weeks. Afterwards, the liquid and solid phases were taken, as described above and analyzed in the same way as the samples for the solubility measurements. Additionally, PXRD measurements were performed of the initial mixtures (1) and (2).

Sublimation of amino acids: The samples of V_3L, produced by liquid-assisted grinding of 3:1 L-Val/L-Leu for 60 min with 0.05 µL mg^{-1} added water, were added to a vacuum tube, and the pressure was reduced to 300 mbar. Pressure and temperature during sublimation were loosely guided by procedures described for amino acid studies in the literature [24–26]. At the top part of the vacuum tube, a cold finger at ~20 °C was used for recrystallization. The sample was then heated by an oil bath to either 142 °C or 152 °C. As soon as crystallization was observed on the cold finger, the sublimation was stopped, and the crystals were collected. Afterwards, the sublimation was continued for 3 h at a constant temperature, and the crystals were again collected. The crystals and the unsublimated residue were then analyzed by PXRD measurement.

2.3. Analytical Techniques

High-Performance Liquid Chromatography (HPLC): For HPLC analysis, an Agilent 1200 system, equipped with a Phenomenex Chirex® 3126 (D)-penicillamine column (length: 50 mm; diameter: 4.6 mm), was used to measure the concentration and amino acid composition of the samples. The samples were dissolved in the eluent, a 2 millimolar aqueous copper sulfate solution mixed with methanol at a 90/10 vol.% composition, to a maximum concentration of 0.03 wt.%. Then, 3 µL samples were injected at an eluent flow rate of 0.5 mL min^{-1} and were analyzed at 25 °C and a wavelength of 260 nm.

Powder X-Ray Diffractometry (PXRD): To investigate the solid phase behavior and to validate the formation of solid solution and co-crystals, powder X-ray diffraction was used. For this, samples obtained from various experiments were measured on background-free sample holders in a PANalytical X'Pert Pro diffractometer using $Cu_{K\alpha}$ radiation in a 2θ range from 4 to 32° with a step size of 0.0167° and a scanning time of 200 s per step. The resulting patterns were normalized to their highest intensity to improve their comparability.

2.4. Computational Details

All calculations were performed with TURBOMOLE (Turbomole GmbH, version 7.6, Karlsruhe, Germany) [27,28] using the B97-D [29] and TPSS [30] exchange-correlation functions with a D3 dispersion term and Becke-Johnson Damping [31]. For all calculations, the "def2-TZVPP" basis sets by Ahlrichs and coworkers were used [32] in the resolution-of-identity approximation with suitable auxiliary basis sets [33,34]. The fitting of the Coulomb density and continuous fast multipole methods (CFMM) [35,36] makes it possible to calculate the energies and perform structural optimizations using atom-centered Gaussian basis functions for molecular and periodic systems on the same grounds. For calculations on very large molecular systems, a low-memory modification of the RI approximation was implemented in the riper module [37]. Thus, the lattice energy can be directly calculated using the same atom-centered Ahlrichs' Gaussian basis functions as the energy difference between the ideal solid state and the ideal isolated, fully relaxed molecule in the gas phase. The periodic DFT implementation in Turbomole makes use of a Γ-point centered mesh of k points. In 3D periodic systems, each sampling point is defined by its components k_1, k_2, and k_3 along the reciprocal lattice vectors $\mathbf{b_1}$, $\mathbf{b_2}$, and $\mathbf{b_3}$

$$k = k_1\mathbf{b_1} + k_2\mathbf{b_2} + k_3\mathbf{b_3}. \quad (1)$$

The unit cell is the smallest non-repetitive representation of the crystal. It contains all symmetry inequivalent atoms. Calculations at the gamma point (1 × 1 × 1 k-points) do not consider interactions with other atoms from neighboring unit cells. The 3 × 3 × 3 k-points specify the unit cell surrounded by the adjacent replicates of the cell, and interactions with atoms from neighboring unit cells are taken into account. It could be shown that a k-point sampling of 3 × 3 × 3 is necessary to achieve a convergence of lattice energies for molecular crystals [18].

The lattice energy, E_{latt}, is defined as the energy difference between a static, perfect, infinite crystal (ideal static solid, *iss*) and its related ideal static gas (*isg*) of non-interacting molecules in their lowest energy conformation at 0 K (Equation (2) where Z is the number of molecules in the unit cell).

$$E_{latt} = E^{iss}/Z - E^{isg}. \quad (2)$$

The lattice energy is a measure of the energy released by the individual molecules which are associating and forming a crystal. It is thus a quantitative description of the interactions in the solid state and has a negative sign.

3. Results and Discussion

3.1. Solution Behavior of the V_3L Compound in Water and Water–Ethanol Mixtures: The Ternary L*-Val/*L*-Leu/Solvent System*

Solubilities of L-Val and L-Leu mixtures in water and in various water/antisolvent mixtures were reported in previous works [9–11]. These studies show that the decrease in the solubility by the addition of ethanol as an antisolvent has a bigger effect on L-Val than it has on L-Leu. Figure 1 shows the ternary solubility phase diagram of L-Val and L-Leu in (a) water and (b) a water/ethanol (84/16 mol.%) mixture at 25 °C. The data sets were determined by the methods explained in the experimental procedure section above. The diagram reveals solubility maxima at 88/12 mol.% L-Val/L-Leu in water and 80/20 mol.% L-Val/L-Leu composition in the 84/16 mol.% water/ethanol mixture as solvent. This shift in the maximum solubility can be attributed to the solubility behavior of the pure components with a rising ethanol content in the solvent. The same is true for acetone and isopropanol [11]. Since the overall behavior of the system is qualitatively similar, only results for ethanol are shown here. Additionally, it is shown that the maximum solubility is closer to the L-Val side than the isopleth of the V_3L compound at its molecular composition of 75:25 mol.% L-Val/L-Leu (see dashed line) for both cases. Unlike the V_2I compound found in the L-Val/L-Ile system [8,22,38], this system does not show a local solubility minimum at the V_3L compounds' composition and, consequently, exhibits full miscibility

of the two amino acids at the solid state under the conditions applied (used solvent/solvent mixture, temperature). Thus, either the formation of the V_3L co-crystal does not lead to a co-crystal typical local solubility minimum or the minimum with its corresponding local eutectics [22] are in very close proximity to each other at the solubility maximum. In both cases, the behavior of this system can be treated as an alyotropic [39] continuous solid solution in the liquid phase, as demonstrated in our previous works [9–11].

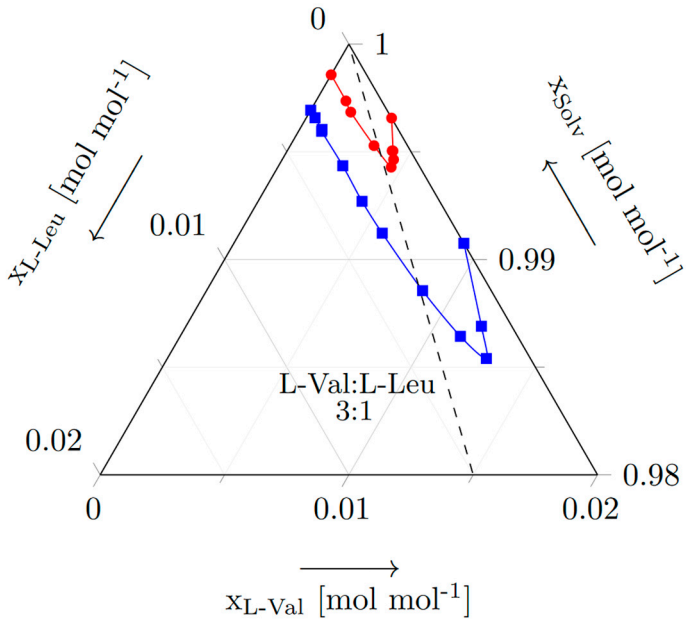

Figure 1. Ternary phase diagram of L−Val and L−Leu in (blue, ■) water and (red, ●) water/ethanol (84/16 mol%) as solvent. Data were acquired by solubility experiments performed at 25 °C. Dashed line: Isopleth of the V_3L co-crystal. Figure adapted from [9,10].

Figure 2 shows selected plots of PXRD measurements of the solid phases from the solubility experiments. Blue lines represent experiments conducted in pure water, and red lines show the water/ethanol experiments. The black line is a calculated single crystal diffractogram of V_3L obtained from CDCC LENGAP02. Characteristic small peaks of V_3L can be seen in the blue plots roughly at an angle of 20°. These peaks are missing in data collected for the mixed solvent phase containing water and ethanol. Biphasic behavior can be seen in all measured data sets at an angle of 14 to 16°. Comparable diffractograms were measured for solid phases obtained from water/isopropanol and water/acetone mixtures via antisolvent crystallization [11]. V_3L was present regardless of the composition of the solvent phase. This could be explained by faster equilibration during antisolvent crystallization as opposed to evaporative crystallization in a rotary evaporator, which, due to a slower crystallization rate, results in larger crystals, which take longer to equilibrate. This leads to the hypothesis that V_3L is a metastable compound.

3.2. Verification of V_3L Phase Behavior via Mechanochemistry, Slurry, and Sublimation Studies

To test the above hypothesis, the V_3L compound was first manufactured by liquid-assisted grinding of L-Val and L-Leu mixtures in a grinding mill. This forces "molecular mixing" and, thus, the formation of solid solutions and/or V_3L by introducing energy into the system. Figure 3 shows the PXRD diffractograms of a physical 3:1 mixture of L-Val and L-Leu, ground for 30 mins with varying amounts of added water. Additionally, the powder patterns of the initial physical mixture and the calculated plot of the V_3L are shown. It can be seen that, without the addition of water, the solid solution and V_3L formation were not possible, and a partly amorphous structure was obtained. However, in the presence of water, the addition of a smaller amount of water provides a larger fraction of V_3L instead of the related solid solution. Since large amounts of pure L-Val excesses could be found

in almost all measured samples (at an angle of ~7.5°), the formed solid solutions are of the V_3L/L-Leu type (seen between 6 and 7° 2θ). The samples prepared with 0.05, 0.1, and 0.6 µL/mg water are shown to be triphasic since a small content of the L-Leu phase is present, too, which was not completely transformed by grinding.

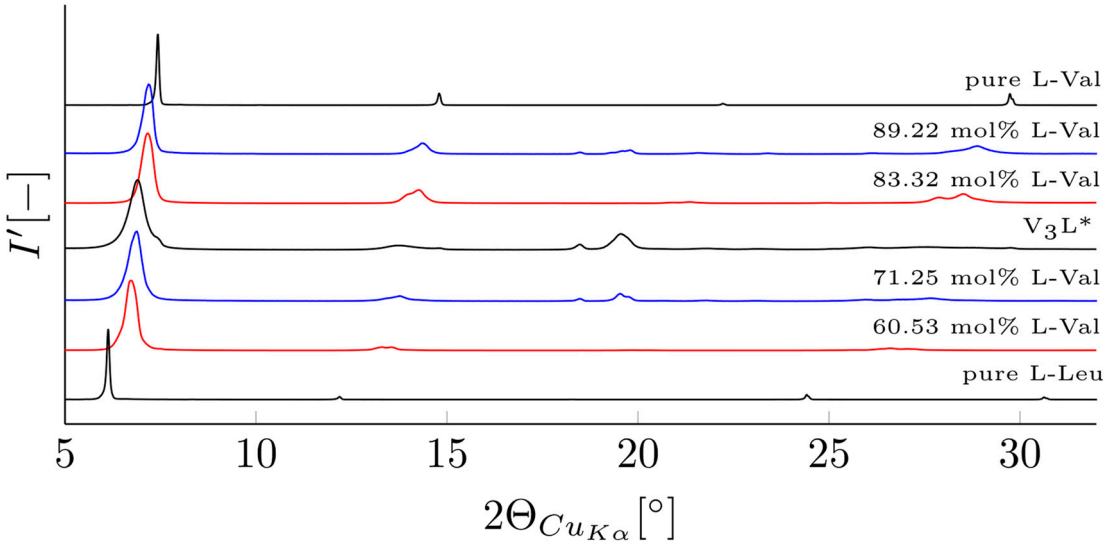

Figure 2. Selected PXRD patterns of various solid phases gathered during solubility experiments at 25 °C. Adapted from to [10]. Blue: water as solvent phase; Red: water/ethanol (84/16 mol.%) as solvent phase; black, *: Calculated diffractogram according to CDCC LENGAP02.

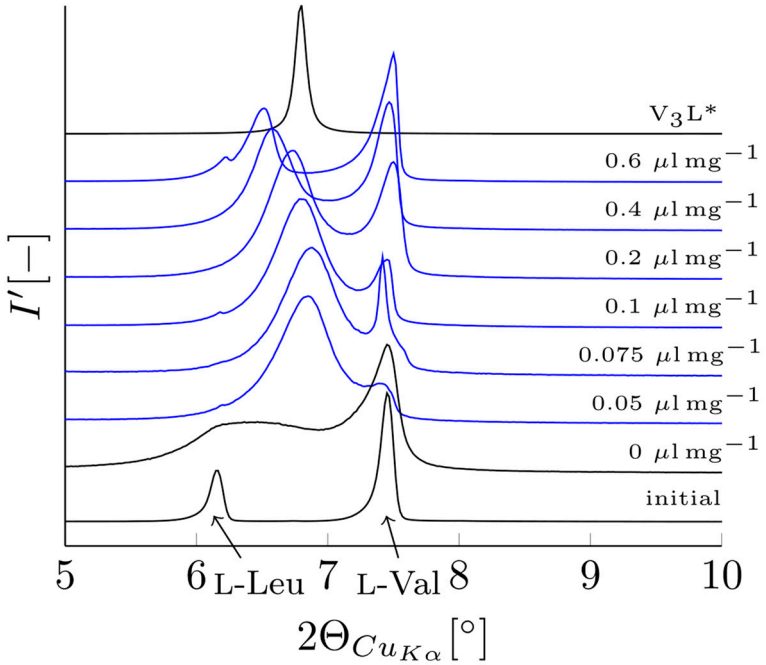

Figure 3. Characteristic part of the diffractograms of the 3:1 L-Val:L-Leu sample ground with various amounts of added water. Ground for 30 min at 25 Hz. The initial PXRD patterns before grinding and a calculated diffractogram of V_3L (V_3L *) respectively.

To further study the effect the solvent has on the formation of V_3L, additional grinding experiments were performed using varying amounts of ethanol as a solvent. Figure 4 shows the resulting diffractograms after a grinding time of 30 mins with ethanol.

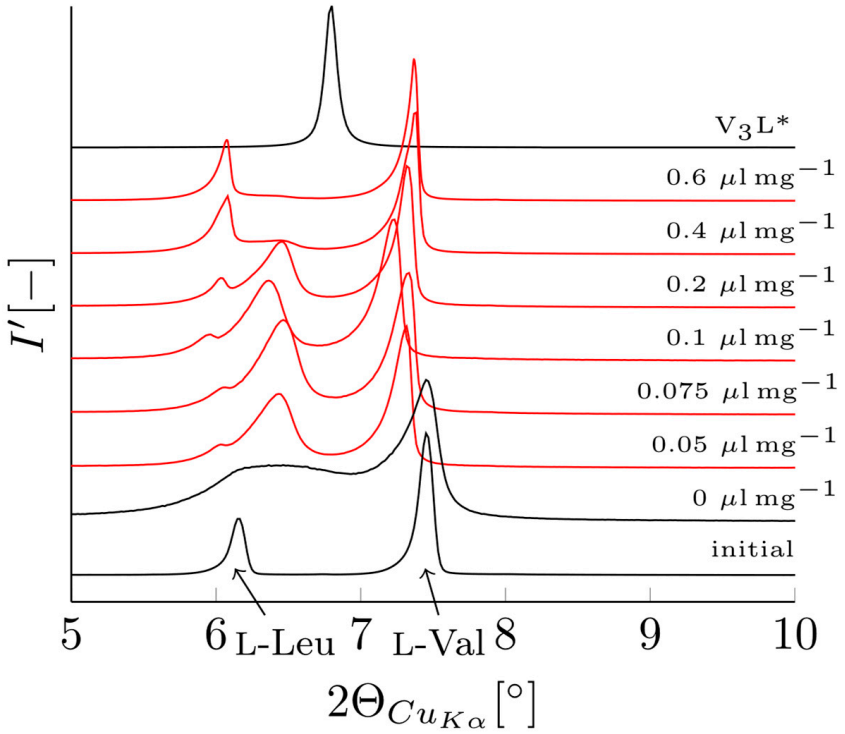

Figure 4. Characteristic part of the diffractograms of the 3:1 L-Val:L-Leu sample ground with various amounts of added ethanol. Ground for 30 min at 25 Hz. The initial PXRD patterns before grinding and a calculated diffractogram of V_3L (V_3L *) are provided at the bottom and top, respectively.

L-Val and L-Leu show the increasing formation of V_3L with a decreasing amount of solvent present during grinding. If more solvent is present during the grinding process, the equilibration between the solid and liquid phases is accelerated, while equilibration during experiments with small amounts of solvent is slower. Thus, the V_3L co-crystal again appears to be metastable since lower amounts of solvent favor the crystallization of this phase. Additionally, a larger solvent fraction decreases the friction between the particles, resulting in less energy supplied to the solid phase and a slower phase transition. This could be a reason for the reduced V_3L formation at higher solvent fractions. However, in the presence of ethanol, a lower overall amount of V_3L is formed as compared to the experiments with water-assisted grinding (see Figure 3). At higher amounts of ethanol, virtually no V_3L was formed. Therefore, it can be concluded that, due to the higher solubility of the amino acids in water compared to ethanol, the formation of V_3L is driven by liquid phase mass transfer.

In Figure 5, the influence of the grinding time on V_3L formation when only adding minimal amounts of water is shown. It is seen that the pure L-Val fraction decreases with increasing grinding time, clearly visible at the peaks at 7.5 and 15 °. After 60 mins of grinding, only a residual fraction of pure L-Val and L-Leu was found. The results show that an increase in the grinding time, which increases the energy supplied to the system, favors the formation of V_3L. Additionally, longer grinding times (up to 60 min) do not yield amorphous solid phases, which would indicate an excess of energy supplied to the system. Sufficiently pure V_3L was obtained by grinding for 60 mins upon the addition of 0.05 µL mg^{-1} water.

To further investigate the (meta)stability of V_3L in its corresponding saturated (equilibrium) solution, slurry experiments of different initial phases containing L-Val and L-Leu in a 3:1 composition were performed. After an equilibration time of three weeks, the prepared samples were analyzed by PXRD analysis. The results are shown in Figure 6.

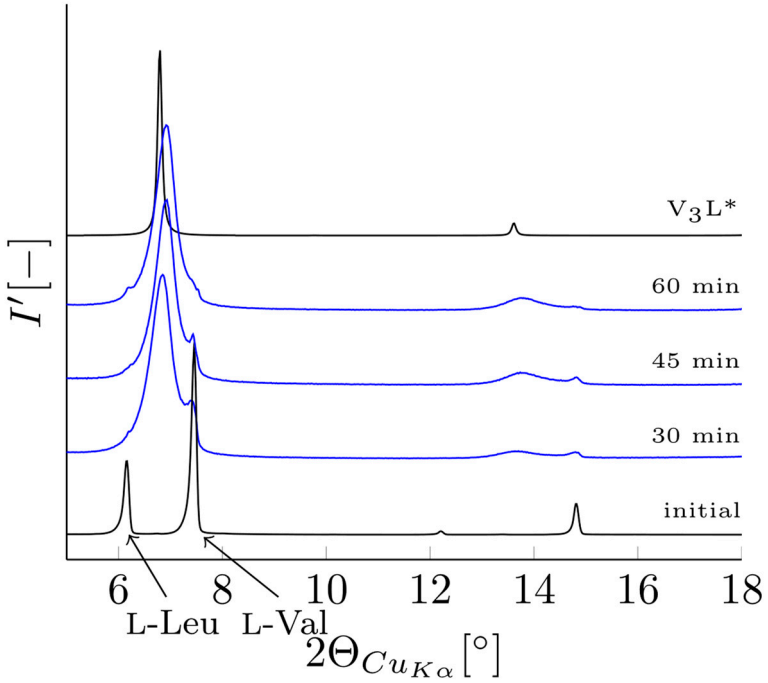

Figure 5. Diffractograms of 3:1 L-Val:L-Leu samples ground with 0.05 µL mg^{-1} added water at 25 Hz for various durations. The initial physical mixture and a calculated diffractogram of V_3L (V_3L *) are shown as well.

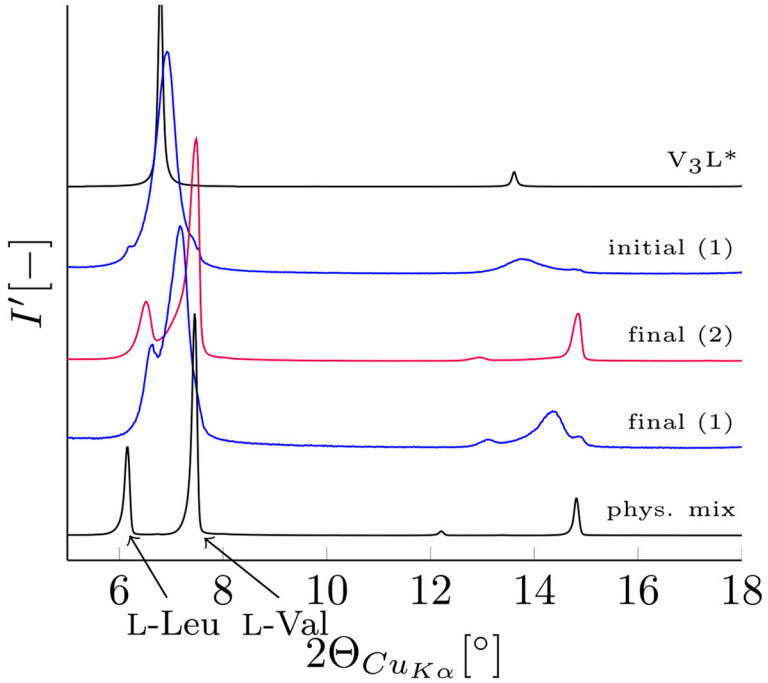

Figure 6. Diffractograms of slurry experiment samples after equilibration for 3 weeks. (1) V_3L compound obtained by grinding; (2) 50:50 wt.% mixture of (1) and a 3:1 L-Val/L-Leu physical mixture. Initial state of the 3:1 mixture and the calculated diffractogram of V_3L (V_3L *) are shown for comparison.

In the almost pure V_3L sample (1), V_3L is present in solid solutions with both L-Val and L-Leu, i.e., a clear decrease of the pure V_3L fraction is observed. Without this reduction, the solid solutions would not have been formed. Sample (2), which was a 50:50 wt.% mixture of pure L-Val and L-Leu and V_3L, shows a clear transition of the V_3L

phase into the two specific solid solutions based on pure L-Val and L-Leu. Two distinct phases are observed in the diffractogram at the angles of 6.5 and 7.5° as well as 13 and 15° corresponding to solid solutions consisting of L-Val/V_3L and L-Leu/V_3L, respectively. The formation of two separate solid solutions indicates at least one miscibility gap within this system. These solid solutions are consistent with previously reported solid solutions formed in this system [9–11,13]. Consequently, pure V_3L, whether initially present or formed during equilibration experiments, was not found in any measured sample (see angles at 7 and 13.5°). Therefore, these slurring studies underline the hypothesis that the V_3L co-crystal is a metastable phase in the L-Val/L-Leu system.

In addition to the slurry experiments, sublimation of the amino acids was performed to investigate a potential purification of V_3L. Figure 7 depicts the resulting PXRD patterns measured before and after the sublimation of the V_3L compound.

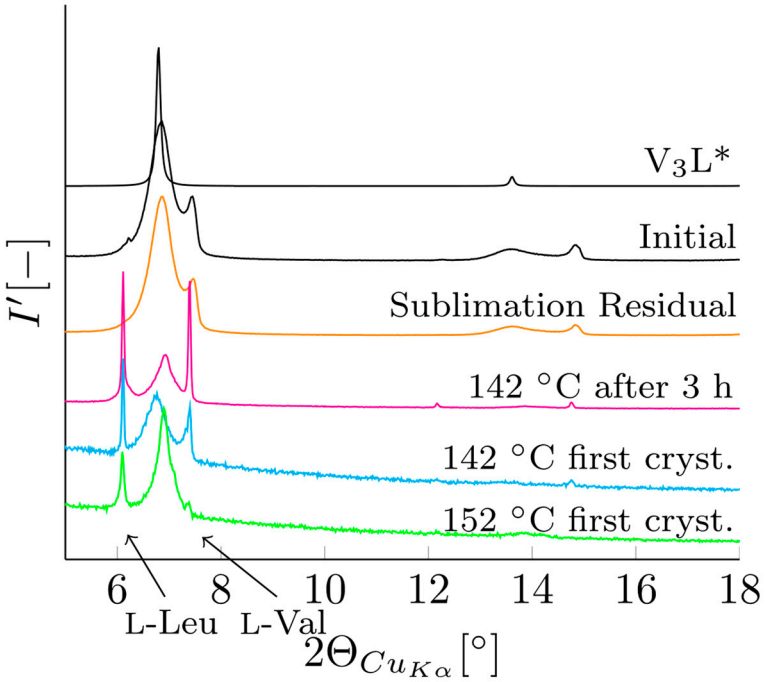

Figure 7. Diffractograms of sublimation experiment samples before sublimation (black), residual (orange), and sublimate (purple) after 3 h sublimation at 142 °C, as well as sublimate at 142 °C (blue) and 152 °C (green) collected directly after crystallization. For comparison, the calculated diffractogram of V_3L (V_3L *) is included.

The diffractograms of samples, which were collected directly after recrystallization (blue and green), were measured with only a small amount of samples. This led to smaller peak intensities relative to the other samples and a higher amount of noise. V_3L (6.5°), L-Val (7°), and L-Leu (6°) were detected in the sublimate collected after first crystallization at 142 °C. In this sample, a slight shift of the V_3L peak to lower angles was observed. Continuation of the sublimation at 142 °C (purple) for 3 h did not change the composition of the sublimate significantly. Analysis of the corresponding residual (orange) verified that all of pure L-Leu, as compared to the initial composition (black), sublimated. This indicates a preferred sublimation of L-Leu, implying a higher vapor pressure when compared to V_3L. In the sample collected at 152 °C (green), L-Val (7°) was only found in small amounts relative to V_3L, while the amount of L-Leu relative to V_3L decreased slightly. Hence, V_3L was obtained with fewer impurities after sublimation at higher temperatures. This can be explained by the rapid increase in L-Val volatility from 142 to 152 °C, which promotes pure V_3L formation. In addition to our results, in [14], unidentified peaks in the PXRD patterns were found in the sublimation of L-Val and L-Leu mixtures, which could be assigned to V_3L.

The sublimation experiments again indicate the metastable behavior of V_3L since a steeper temperature gradient leads to faster crystallization rates and, therefore, tends to form larger amounts of unstable phases. Additionally, L-Leu and L-Val peaks found in all sublimated samples show a very small peak width indicating pure components. Due to the high concentration gradient between the gaseous and solid phases, crystallization occurs in out-of-equilibrated conditions, which inhibits the formation of solid solutions. Since a metastable V_3L is preferred to crystallize as compared to the pure amino acids, the residual fraction of L-Val and L-Leu in the sublimate samples might originate from a shift in the 3:1 ratio in the gaseous phase due to different sublimation rates of L-Val and L-Leu. If complete sublimation of L-Leu is assumed, it will crystallize either as L-Leu or as V_3L, depending on the availability of L-Val in the gaseous phase. In the sample collected at 142 °C, L-Val did not sublimate fast enough; L-Leu is found in comparable quantities as pure L-Leu and V_3L, while excess L-Val crystallizes as a pure component afterwards. At 152 °C, the sublimation was accelerated due to higher temperatures, and L-Leu was predominantly found as V_3L since L-Val sublimated more quickly. Here, only small amounts of pure L-Val crystallized. The lower vapor pressure and the preferred crystallization of V_3L imply its metastability.

3.3. Intermolecular Interactions in the Crystals of the L-Val/L-Leu System

As seen in Figure 8, the crystal structures of L-Val and L-Leu are determined by strong hydrogen bonding interactions between the amine and carboxylate groups. In the gas phase, the neutral form of each amino acid is prevalent. L-Leu crystallizes in a dimer-of-dimers arrangement of molecules in which each of the four molecules in the unit cell forms two electrostatic interactions, plus there is one zwitterionic attraction between the dimers (see Figure 8). For L-Val, one dimer is formed, which undergoes two attractive interactions with the other two monomers in the unit cell.

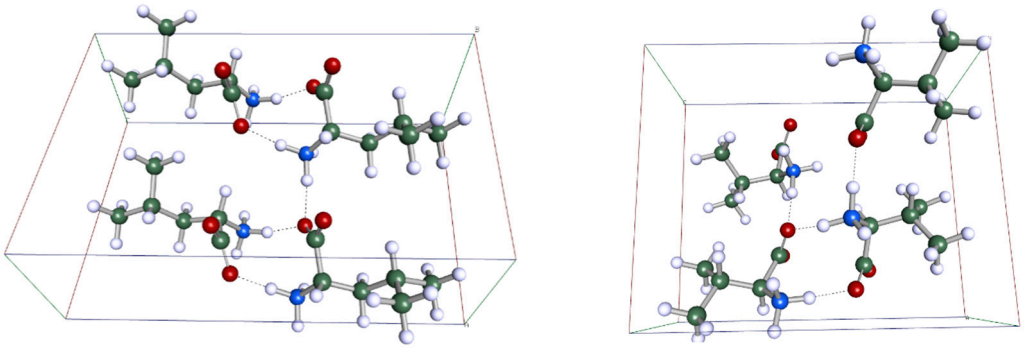

Figure 8. Visualization of hydrogen bonding in crystals of L-Leu (**left**) and L-Val (**right**) indicated by dotted lines.

The experimental heats of sublimation of pure L-Leu and L-Val differ by only ~1 kJ/mol (see Table 1). All calculations for CCDC entries of L-Leu (LEUCIN/LEUCIN01/LEUCIN02/LEUCIN04/LEUCIN05) provided identical lattice energies within 1 kJ/mol and showed the existence of only a single polymorph. The same holds for L-Val (LVALIN01 and LVALIN05). The calculated lattice energies for L-Leu are overestimated by 31 kJ/mol for B97-D and 13 kJ/mol for TPSS-D3. For L-Val, the energy difference is 11 and 10 kJ/mol for B97-D and TPSS-D3, respectively. This order of accuracy is in agreement with previous calculations [18,19] and closer to experimental values.

The published crystal structure of V_3L [8] (CCDC entry LENGAP02) displays structural disorder with equal occupancies (0.5:0.5). Separation of the individual constituents shows a 50% contribution of pure valine (V_4) and 50% of the mixed V_2L_2 crystal providing the overall V_3L ratio. Periodic DFT calculations start from a unit cell with well-defined coordinates of all atoms. We thus created a 'model' for a unit cell with an apparent V_3L composition by substituting one leucine from V_2L_2 with a valine residue (see Figure 9).

Given the very similar binding modes in the pure L-amino acid crystals in Figure 8, this appears plausible. The investigation of all possible and arbitrary arrangements of three valine and one leucine molecule in a unit cell is still beyond the accurate DFT calculations of lattice energies. In addition, the generation of a very large supercell with an apparent overall V_3L composition and locally different packing modes of valine and leucine residues is impractical.

Table 1. Calculated lattice energies in kJ/mol for L-Leu and L-Val amino acids. Experimental values obtained from [40].

	B97-D3/def2-TZVPP	TPSS-D3/def2TZVPP	Exp.
L-Leucine	−176	−158	−145
L-Valine	−155	−154	−144
V_2L_2	−160	−151	
V_3L	−155	−150	

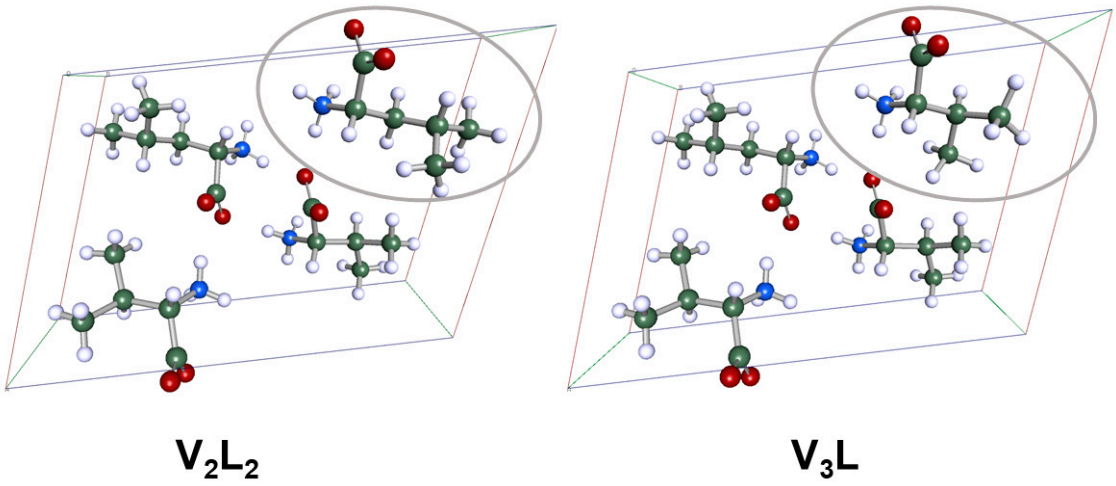

Figure 9. Generation of unit cells and structural arrangement in mixed crystals of L-leucine and L-valine (V_2L_2, (**left**); V_3L, (**right**)).

We thus used periodic DFT calculations of a V_3L model to investigate the thermodynamic difference between different compositions. For V_2L_2 and V_3L, the calculated lattice energies only differed by 5–9 kJ/mol (Table 1). Again, the B97-D results are more negative than those obtained with TPSS-D3. Such a small energy difference implies that crystals of pure L-leucine and L-valine and mixed crystals of L-leucine/L-valine at different compositions cannot be separated based on of thermodynamics and, on the other hand, explains why mixed crystals with varying component ratios are feasible for this system. The packing and the magnitude of interactions for the V_3L co-crystal are very close to that of the pure crystalline L-amino acids. However, a kinetic control of the crystallization process may lead to a metastable V_3L compound.

4. Conclusions

The formation and stability of a V_3L co-crystal in the L-Val/L-Leu amino acid system have been studied. Initial indications of its metastability were derived from solid–liquid equilibria in various aqueous solutions. In such solutions, classical co-crystal phase behavior was not observed, even though V_3L was found in various solid phases. Additionally, in the crystallization-based separation of solid solutions between L-Val and L-Leu, an expected limitation imposed by V_3L was not confirmed, and its influence on the separation could be neglected [10]. Preliminary studies showed the formation of V_3L independent of crystallization conditions, rates, or solvent composition.

More focused, in-depth studies on the co-crystal were initially conducted in an attempt to obtain a purified V_3L compound. For this, liquid-assisted grinding was chosen as its high energy input favors metastable phases under appropriate conditions. During these grinding experiments, a small amount of solvent was required to avoid semi-amorphic phase transitions. Furthermore, it was shown that V_3L formation was favored by lower solvent amounts, higher solubility in the chosen solvent, and longer grinding times. Higher solubility aids in liquid-phase mass transport and indicates a phase transition to V_3L via the liquid phase. Lower solvent amounts and longer equilibration times are proportional to more energy supplied to the solid and, as such favor metastable phases. V_3L was obtained in sufficient purity (see Figure 5) by grinding for 60 min at 25 Hz in the presence of 0.05 µL min^{-1}. The obtained V_3L was used further for slurry equilibration and sublimation experiments. During the slurry equilibration, a decrease in V_3L in favor of L-Val- or L-Leu-based solid solutions was observed, which verifies solid solutions as being the stable solid-state form in this binary system. Likewise, in out-of-equilibrium conditions, as present during the sublimation experiments performed, V_3L was found alongside smaller fractions of pure L-Val and L-Leu at 142 and 152 °C. Here, no solid solutions were observed. Again, these studies support the hypothesis of a metastable V_3L compound.

Hence, the definitely proven metastability of V_3L is the reason that its existence does not hinder crystallization-based purification of the L-Val/L-Leu system under near-equilibrium conditions, as verified in previous works [10]. However, further studies need to be performed to quantify V_3L's impact under non-equilibrium, kinetically controlled crystallization.

To support the experimental results, QM calculations of the various solid forms were performed, and their crystal lattice energies were calculated. The results for pure L-Leu and L-Val were in excellent agreement with experimental results available in the literature. Further calculations showed no significant difference between the lattice energies of pure L-Val and L-Leu, V_2L_2, and a model V_3L system. This not only supports the continuous miscibility exhibited in this system but also the thermodynamic metastability of V_3L, and its existence in numerous samples during own and experiments from other groups [8–11,14]. This can now be attributed to the small difference in the V_3L lattice energy when compared to the solid solution and the pure compounds.

This indistinguishable thermodynamic difference requires further in-depth and accurate investigations with considerable experimental effort. In particular, sublimation studies covering a broader temperature range could be further exploited to gain insight into the stability of V_3L. Additionally, the conditions can be specifically tailored to acquire potentially pure V_3L for further investigations. Other conditions or solvents and their effects on the metastability and transition kinetics can also be investigated.

In conclusion, the results presented in this work demonstrate a clear metastability of V_3L, which explains its negligible influence on crystallization-based separation for the L-Val/L-Leu system under the conditions used. Additionally, this work shows how a previously unknown complex phase behavior can be exhibited even by well-studied systems. Such diversity of phase behavior in a simple but biologically and geologically relevant amino acid system opens up further opportunities for research.

Author Contributions: Conceptualization, V.T. and H.L.; Methodology, V.T., M.S. and H.L.; Formal analysis, V.T., M.S. and H.L.; Investigation, V.T. and M.S.; Resources, H.L. and M.S.; Writing—original draft, V.T.; Writing—review & editing, V.T., M.S. and H.L.; Supervision, H.L.; Funding acquisition, M.S. All authors have read and agreed to the published version of the manuscript.

Funding: This research was supported by the Max Planck Society for the Advancement of Science. This work is part of the Research Initiative "SmartProSys: Intelligent Process Systems for the Sustainable Production of Chemicals" funded by the Ministry for Science, Energy, Climate Protection, and the Environment of the State of Saxony-Anhalt.

Data Availability Statement: Data sharing is not applicable to this article.

Acknowledgments: We thank Elena Kotelnikova and Anton Isakov (Department of Crystallography, Saint Petersburg State University) for the initial discussions and collaboration in this project. Additionally, the support of Jacqueline Kaufmann and Stefanie Oberländer in HPLC and PXRD measurements and the sublimation experiments is acknowledged.

Conflicts of Interest: The authors declare no conflict of interest.

References

1. Myerson, S. *Handbook of Industrial Crystallization*; Butterworth Heinemann: Oxford, UK, 2002.
2. Kotelnikova, E.N.; Isakov, A.I.; Lorenz, H. Non-equimolar discrete compounds in binary chiral systems of organic substances. *CrystEngComm* **2017**, *19*, 1851–1869. [CrossRef]
3. Hilfiker, R. Polymorphism of Crystalline, Systems. In *Crystallization: Basic Concepts and Industrial Applications*; Beckmann, W., Ed.; Wiley: Hoboken, NJ, USA, 2013; pp. 85–103.
4. Lusi, M. A rough guide to molecular solid solutions: Design, synthesis and characterization of mixed crystals. *CrystEngComm* **2018**, *20*, 7042–7052. [CrossRef]
5. Kitamura, M. Polymorphism in the crystallization of L-glutamic acid. *J. Cryst. Growth* **1989**, *96*, 541–546. [CrossRef]
6. Gónzalez, L.J.; Shimizu, T.; Satomi, Y.; Betancourt, L.; Besada, V.; Padrón, G.; Orlando, R.; Shirasawa, T.; Shimonishi, Y.; Takao, T. Differentiating α- and β-aspartic acids by electrospray ionization and low-energy tandem mass spectrometry. *Rapid Commun. Mass. Spectrom.* **2000**, *14*, 2092–2102. [CrossRef] [PubMed]
7. Sadovnichii, R.; Kotelnikova, E.; Lorenz, H. Thermal Deformations of Crystal Structures in the L-Aspartic/L-Glutamic Acid System and DL-Aspartic Acid. *Crystals* **2021**, *11*, 1102. [CrossRef]
8. Isakov, I.; Lorenz, H.; Zolotarev, A.A., Jr.; Kotelnikova, E.N. Heteromolecular compounds in binary systems of amino acids with opposite and same chiralities. *CrystEngComm* **2020**, *22*, 986–997. [CrossRef]
9. Sadeghi, M.; Tenberg, V.; Münzberg, S.; Lorenz, H.; Seidel-Morgenstern, A. Phase Equilibria of L-Valine/L-Leucine Solid Solutions. *J. Mol. Liq.* **2021**, *340*, 117315. [CrossRef]
10. Tenberg, V.; Sadeghi, M.; Seidel-Morgenstern, A.; Lorenz, H. Bypassing thermodynamic limitations in the crystallization-based separation of solid solutions. *Sep. Purif. Technol.* **2022**, *283*, 120169. [CrossRef]
11. Tenberg, V.; Hokmabadi, M.; Seidel-Morgenstern, A.; Lorenz, H.; Sadeghi, M. Investigation of the Antisolvent Effect on the Phase Behavior of Amino Acid Solid Solutions. *Ind. Eng. Chem. Res.* **2023**, *62*, 753–761. [CrossRef]
12. Daltrup, J.-B.G.; Held, C.; Ruether, F.; Schembecker, G.; Sadowski, G. Measurement and Modeling Solubility of Aqueous Multisolute Amino-Acid Solutions. *Ind. Eng. Chem. Res.* **2010**, *49*, 1395–1401. [CrossRef]
13. Kurosawa, I.; Teja, A.S.; Rousseau, R.W. Solid-liquid equilibria in L-leucine + L-valine + water. *Fluid Phase Equilibr.* **2005**, *228–229*, 83–87. [CrossRef]
14. Viedma, C.; Ortiz, J.E.; de Torres, T.; Cintas, P. Enantioenrichment in sublimed amino acid mixtures. *Chem. Commun.* **2012**, *48*, 3623–3625. [CrossRef] [PubMed]
15. Reilly, A.M.; Tkatchenko, A. Understanding the role of vibrations, exact exchange, and many-body van der Waals interactions in the cohesive properties of molecular crystals. *J. Chem. Phys.* **2013**, *139*, 024705. [CrossRef]
16. Dolgonos, G.A.; Hoja, J.; Boese, A.D. Revised values for the X23 benchmark set of molecular crystals. *Phys. Chem. Chem. Phys.* **2019**, *44*, 24333–24344. [CrossRef] [PubMed]
17. Otero-de-la-Roza, A.; Johnson, E.R. A benchmark for non-covalent interactions in solids. *J. Chem. Phys.* **2012**, *137*, 054103. [CrossRef]
18. Buchholz, H.K.; Stein, M. Accurate lattice energies of organic molecular crystals from periodic turbomole calculations. *J. Comput. Chem.* **2018**, *39*, 1335–1343. [CrossRef]
19. Stein, M.; Heimsaat, M. Intermolecular Interactions in Molecular Organic Crystals upon Relaxation of Lattice Parameters. *Crystals* **2019**, *9*, 665. [CrossRef]
20. Otero-de-la-Roza, A.; Cao, B.H.; Price, I.K.; Hein, J.E.; Johnson, E.R. Predicting the Relative Solubilities of Racemic and Enantiopure Crystals by Density-Functional Theory. *Angew. Chem. Int. Ed.* **2014**, *53*, 7879–7882. [CrossRef] [PubMed]
21. Geatches, D.; Rosbottom, I.; Robinson, R.L.M.; Byrne, P.; Hasnip, P.; Probert, M.I.J.; Jochym, D.; Maloney, A.; Roberts, K.J. Off-the-shelf DFT-DISPersion methods: Are they now "on-trend" for organic molecular crystals. *J. Chem. Phys.* **2019**, *151*, 044106. [CrossRef]
22. Isakov, A.I.; Kotelnikova, E.N.; Münzberg, S.; Bocharov, S.N.; Lorenz, H. Solid Phases in the System L-Valine—L-Isoleucine. *Cryst. Growth Des.* **2016**, *16*, 2653–2661. [CrossRef]
23. Raza, S.A.; Schacht, U.; Svoboda, V.; Edwards, D.P.; Florence, A.J.; Pulham, C.R.; Sefcik, J.; Oswald, I.D.H. Rapid Continuous Antisolvent Crystallization of Multicomponent Systems. *Cryst. Growth Des.* **2018**, *18*, 210–218.
24. Viedma, C.; Noorduin, W.L.; Oritz, J.E.; de Torres, T.; Cintas, P. Asymmetric amplification in amino acid sublimation involving racemic compound to conglomerate conversion. *Chem. Commun.* **2010**, *47*, 671–673.
25. Lähde, A.; Raula, J.; Malm, J.; Kauppinen, E.I.; Karpinen, M. Sublimation and vapour pressure estimation of L-leucine using thermogravimetric analysis. *Thermochim. Acta* **2009**, *482*, 17–20.

26. Glavin, P.; Bada, J.L. Isolation of Amino Acids from Natural Samples Using Sublimation. *Anal. Chem.* **1998**, *70*, 3119–3122. [PubMed]
27. TURBOMOLE V7.5 2019, University of Karlsruhe and Forschungszentrum Karlsruhe GmbH, 1989–2007, TURBOMOLE GmbH, since 2007. Available online: https://www.turbomole.com (accessed on 24 October 2023).
28. Furche, F.; Ahlrichs, R.; Hattig, C.; Klopper, W.; Sierka, M.; Weigend, F. Turbomole. *Interdiscip. Rev. Comput. Mol. Sci.* **2014**, *4*, 91–100.
29. Grimme, S.; Antony, J.; Ehrlich, S.; Krieg, H. A consistent and accurate ab initio parametrization of density functional dispersion correction DFT-D for the 94 elements H-Pu. *J. Chem. Phys.* **2010**, *132*, 154104.
30. Tao, J.M.; Perdew, J.P.; Staroverov, V.N.; Scuseria, G.E. Climbing the density functional ladder: Nonempirical meta-generalized gradient approximation designed for molecules and solids. *Phys. Rev. Lett.* **2003**, *91*, 146401.
31. Grimme, S.; Ehrlich, S.; Goerigk, L. Effect of the Damping Function in Dispersion Corrected Density Functional Theory. *J. Comput. Chem.* **2011**, *32*, 1456–1465.
32. Wigend, F.; Ahlrichs, R. Balanced basis sets of split valence, triple zeta valence and quadruple zeta valence quality for h to rn: Design and assessment of accuracy. *Phys. Chem. Chem. Phys.* **2005**, *7*, 3297.
33. Eichkorn, K.; Weigend, F.; Treutler, O.; Ahlrichs, R. Auxiliary basis sets for main row atoms and transition metals and their use to approximate coulomb potentials. *Theor. Chem. Acc.* **1997**, *97*, 119–124.
34. Eichkorn, K.; Treutler, O.; Ohm, H.; Haser, M.; Ahlrichs, R. Auxiliary basis-sets to approximate coulomb potentials. *Chem. Phys. Lett.* **1995**, *240*, 283–290, Erratum in *Chem. Phys. Lett.* **1995**, *242*, 652–660. [CrossRef]
35. Łarzarski, R.; Burow, A.M.; Grajciar, L.; Sierka, M. Density functional therory for molecular and periodic systems using density fitting and continuous fast multipole method: Analytical gradients. *J. Comput. Chem.* **2016**, *37*, 2518–2526. [CrossRef]
36. Łazarski, R.; Burow, A.M.; Sierka, M. Density functional theory for molecular and periodic systems using density fitting and continuous fast multipole methods. *J. Chem. Theory Comput.* **2015**, *11*, 3029–3041.
37. Grajciar, L. Low-memory iterative density fitting. *J. Comput. Chem.* **2015**, *36*, 1521–1535. [PubMed]
38. Kotelnikova, E.; Isakov, A.; Lorenz, H. Thermal deformations of crystal structures formed in the systems of malic acid enantiomers and L-valine-L-isoleucine enantiomers. *CrystEngComm* **2018**, *20*, 2562–2572.
39. Prieto, M. Thermodynamics of Solid Solution-Aqueous Solution Systems. *Rev. Mineral. Geochem.* **2009**, *70*, 47–85.
40. Dorofeeva, O.V.; Ryzhova, O.N. Gas-phase enthalpies of formation and enthalpies of sublimation of amino acids based on isodesmic reaction calculations. *J. Phys. Chem. A* **2014**, *118*, 3490–3502. [PubMed]